applied sciences

MDPI

Review

The Application of Microplasma in the Terahertz Field: A Review

Yue Guo, Shuqun Wu *, Xuhui Liu, Lu Yang and Chaohai Zhang

College of Automation Engineering, Nanjing University of Aeronautics and Astronautics, Nanjing 211106, China; guoyue@nuaa.edu.cn (Y.G.); liuxuhui@nuaa.edu.cn (X.L.); ylu@nuaa.edu.cn (L.Y.); zhangchaohai@nuaa.edu.cn (C.Z.)

* Correspondence: wushuqun@nuaa.edu.cn

Abstract: Terahertz functional devices are essential to the advanced applications of terahertz radiation in biology and medicine, nanomaterials, and wireless communications. Due to the small size and high plasma frequency of microplasma, the interaction between terahertz radiation and microplasma provides opportunities for developing functional terahertz devices based on microplasma. This paper reviews the applications of microplasma in terahertz sources, terahertz amplifiers, terahertz filters, and terahertz detectors. The prospects and challenges of the interdisciplinary research between microplasma and terahertz technology are discussed.

Keywords: microplasma; terahertz filter; terahertz amplification; terahertz detection; terahertz source

Citation: Guo, Y.; Wu, S.; Liu, X.; Yang, L.; Zhang, C. The Application of Microplasma in the Terahertz Field: A Review. *Appl. Sci.* **2021**, *11*, 11858. https://doi.org/10.3390/app112411858

Academic Editor: Xinpei Lu

Received: 18 November 2021
Accepted: 7 December 2021
Published: 14 December 2021

1. Introduction

The field of terahertz (THz) spectroscopy, imaging, and technology has grown dramatically over the last three decades due to its promising THz applications in explosives detection [1,2], biology/medicine [3], wireless communication [4], and radio astronomy [5]. The THz frequency range generally refers to the 0.1–10 THz range, which is between microwaves and infrared light in the frequency band [4,6]. With photon energies in the meV range, THz radiation interacts strongly with matters that have characteristic lifetimes in the picosecond range and energetic transitions in the meV range, such as absorption resonances of molecules, chemical reactions, dielectric relaxation and vibrational spectroscopy of liquids, weak collective excitations in solids, and biomolecular collective motions [7]. These characteristics make THz radiation a unique tool for numerous applications. For example, THz radiation does not ionize molecules because of its low energy, presenting a significant advantage in medical imaging over X-rays [8]. THz spectroscopy can act as spectroscopic fingerprints for material identification because molecular crystals possess vibrational absorption bands in the THz range [9]. Compared with microwave frequencies, the THz spectral region offers a higher available bandwidth, which could meet the ever-growing demand for higher data transfer rates in wireless communications [10]. THz images also have the advantage of superior spatial resolution due to the shorter wavelength [11]. Compared with infrared frequencies, many common materials are relatively transparent for THz radiation to penetrate, including common packaging materials such as paper, plastics, and composites [1]. The THz region has been considered the last remaining scientific gap in the electromagnetic spectrum, which is underdeveloped but ripe for exploitation. One of the fundamental reasons is the lack of many functional devices in the THz frequency range.

Terahertz sources, amplifiers, filters, and detectors are necessary functional devices in THz spectroscopy, imaging, and technology. Proof-of-concept experiments and simulations have shown that microplasma interacts strongly with the THz radiation, making it possible to be part of THz functional devices. Microplasma sources have been applied to light sources, material processing, plasma medicine, and electromagnetic wave control [12]. Microplasma usually refers to a plasma with a feature size of less than 1 mm. Atmospheric pressure microplasma is of high electron density and low gas temperature. Due to its

plasma frequency in the terahertz range and featured size, microplasma is well suited to interact with THz radiation in principle [13]. The relative plasma permittivity is dependent on the plasma frequency, the frequency of incident electromagnetic waves, and the collision frequency between electrons and molecules or atoms, which has been described by the well-known Drude model [14]. The relative plasma permittivity is easily tuned by applied voltages or input electric power, which can be positive or negative. From the perspective of dielectrics, microplasma has a nonlinear refractive index and behaves like a metamaterial for THz radiation modulation [15]. It has advantages of fast dynamic response, reconfiguration, and adjustability compared to other methods based on the temperature [16], magnetic field [17], and pressure [18]. At present, extensive works have shown that microplasma plays an important role in THz functional devices, such as THz sources, amplifiers, filters, and detectors. However, although several reviews on the development of THz spectroscopy and imaging [11], THz clinical application [8], THz communication [19], and extreme THz science [20] have been published, there is no overview of microplasma applications in the THz field. Therefore, this work focuses on a few of the recent developments and the implications for the future of microplasma applications in the THz field.

2. Application of Microplasma in THz Functional Devices

2.1. Terahertz Source

The methods of terahertz sources development are usually based on electronics and photonics [21]. From the aspect of electronics, vacuum electronic devices and solid-state semiconductors are usually used. Due to the power and operation frequency limitation of the electronic devices, it is usually hard to obtain a powerful THz source with a frequency spectrum up to tens of THz. From the aspect of photonics sources, photoconductive antenna (PCA), optical rectification, and laser-induced microplasma are usually used [22]. The THz radiation intensity based on PCA is limited by the carrier lifetime. The optical rectification is limited by the nonlinear crystal, which has photon absorption and a damage threshold. THz sources based on laser-induced microplasma have a wide frequency spectrum and no need to worry about the damage threshold of the medium. It allows the operation of THz sources with high-intensity laser input. Therefore, THz sources based on laser-induced microplasma have great potential in generating super terahertz radiation with a wide frequency spectrum.

The THz source based on laser-induced plasma can be used to produce short ultra-broadband pulses covering a broad frequency spectrum reaching well into the infrared, which is essential to identify the spectral "fingerprints" of molecular crystals. The laser-induced plasma has a diameter of 10–100 μm and an electron density of over 10^{17} cm^{-3}. The radiation terahertz spectrum spans from 0.1 to 10 THz, as shown in Figure 1 [23], and the electric field of THz waves is kV/cm~MV/cm [24–27]. With the contribution of a 10 fs laser pulse, a spectrum of the ultrabroadband pulse from far infrared to 200 THz through a plasma is observed, as shown in Figure 2 [28]. In 1993, Hamster et al. first reported the THz generation from the ionized helium gas [29]. A 50 mJ near-infrared pulsed laser is focused on a helium gas target. The helium gas is ionized, resulting in the formation of microplasma with an electron density of 2.5×10^{17} cm^{-3}. The optical-to-THz conversion efficiency is less than 10^{-6}. In 2000, Cook and Hochstrasser improved the infrared–terahertz conversion efficiency, which increases by at least one order of magnitude when an ultrafast laser field composed of the fundamental wave and its second harmonic is used [30]. Classified by the laser wavelength, the two approaches are generally referred to as the "one-color" and "two-color" methods, as shown in Figure 3. A femtosecond or picosecond infrared laser is used to focus on the gas targets. The gases are ionized by the intense laser electric field, resulting in the formation of microplasma. The electrons in microplasma are accelerated with ultrafast oscillation in the strong electric field, radiating broadband electromagnetic waves (including THz waves).

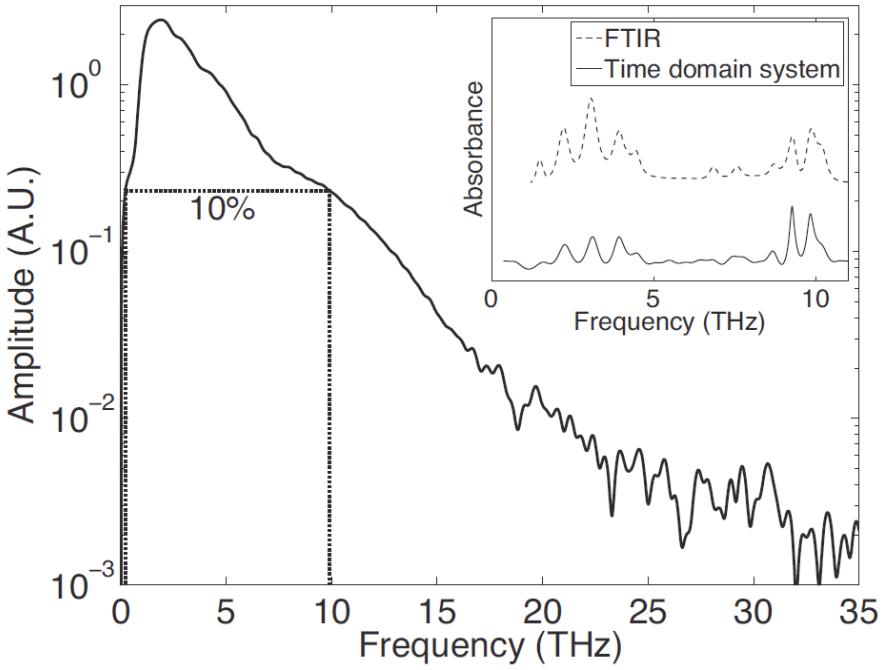

Figure 1. A frequency spectrum covering from 0.1 THz to 35 THz produced by plasma [23].

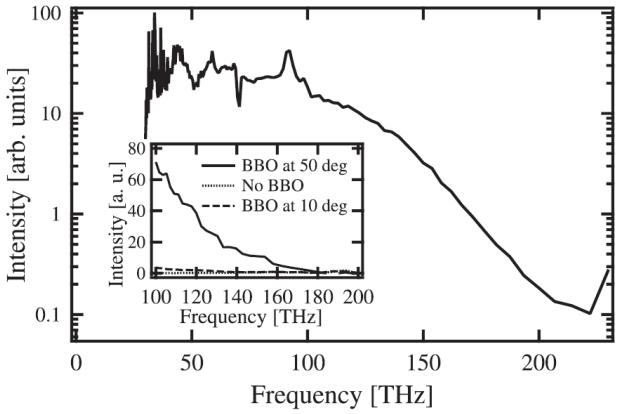

Figure 2. A spectrum of the ultrabroadband pulse from far infrared to 200 THz through a plasma [28].

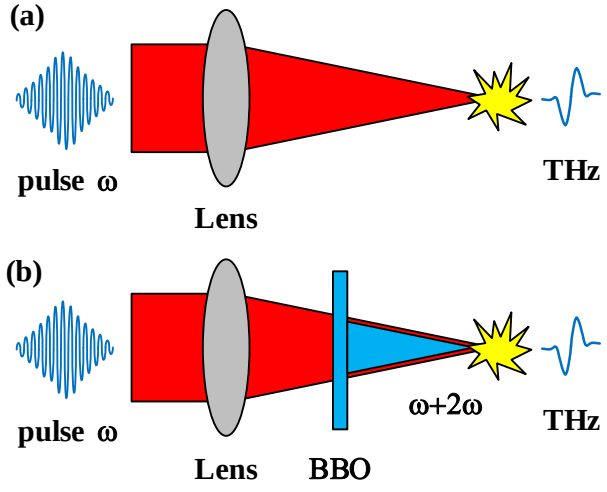

Figure 3. Schematic diagram of laser-induced plasma radiation terahertz wave. (**a**) single-color method; (**b**) two-color method.

In the "one-color" method, the minimum laser pulse energy required to generate measurable THz waveforms is crucial. The laser energy threshold in some previous works is in the range of 30–50 μJ, where the microplasma induced by infrared laser is usually elongated with a radius of tens to hundreds of microns and a length of several millimeters to several centimeters. The estimate scaling law for the THz peak power as a function of the relevant laser source parameters proposed by Hamster et al. is presented as follows:

$$P_{\mathrm{THz}} \propto \frac{(\mathrm{W} \times \mathrm{NA} \times \lambda)^2}{\tau^4} \quad (1)$$

where W is the laser pulse energy, NA is the numerical aperture of the focusing laser cone, λ is the laser wavelength, and τ is the pulse duration. The equation implies that the laser energy threshold can be reduced by increasing NA and the laser intensity at the focal plane. Inspired by this, Fabrizio et al. reported an ambient air laser-induced microplasma as a THz emitter, as shown in Figure 4. The laser beam is focused by a high-NA microscope objective lens into ambient air, generating a microplasma with dimensions of less than 40 μm. [31,32]. The electron density reaches as high as 10^{18} cm^{-3}. The required laser pulse energy is as low as less than 1 μJ. In 2018, they further demonstrated that the microplasma approach could reduce the necessary optical pulse energy by five orders of magnitude while still obtaining a comparable signal-to-noise ratio for THz time-domain spectroscopy [33]. Herein, the electron density of the microplasma should reach up to 10^{19} cm^{-3} or more. The THz radiation is usually a forward propagating cone. As the size of the plasma decreases, the divergence angle increases. For microplasma of fewer than 40 μm, the THz radiation direction is orthogonal to the optical path. In addition, it should be mentioned that the THz generation process is tightly reliant on the characteristics of microplasma, including the size of microplasma, the electron density, the gas pressure, and the gas composition [34,35]. For example, Sheng et al. found that the gas length can tune the shape of the THz waveform and while the amplitude of the THz radiation is constant, which provides a new pathway for terahertz radiation control. In addition, their simulated results show that the THz radiation can be controlled by changing the strength and direction of an external dc magnetic field with a few teslas, and the maximum energy conversion efficiency is doubled in the magnetized plasmas [36].

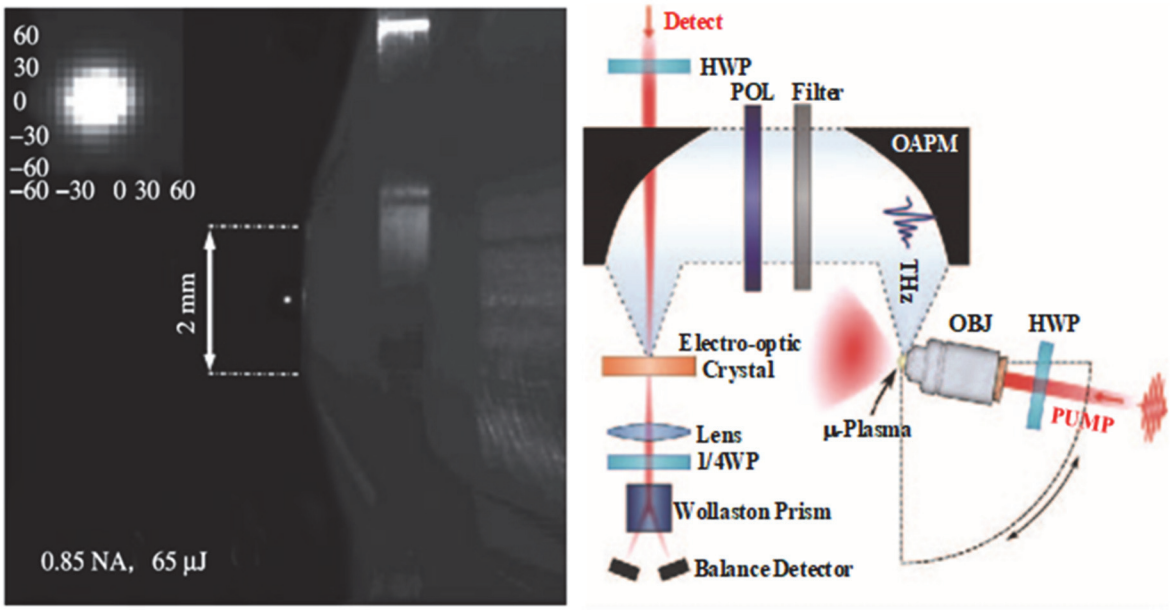

Figure 4. Schematic diagram of laser-induced plasma generation and detection of terahertz waves [30].

In the "two-color" method, the femtosecond laser-induced microplasma has a greater degree of freedom for THz radiation regulation than the "one-color" method. Thiele et al.

simulated the formation of terahertz radiation from microplasma induced by a two-color femtosecond laser [37]. A microplasma with a length of about 10 μm and a thickness of about 1 μm is generated. The argon gas is completely ionized at the focal plane, and the peak electron density reaches 3×10^{19} cm^{-3}. The decrease in the thickness of the microplasma layer is beneficial to improve the optical-to-THz conversion efficiency. The efficiency is above 10^{-4} for 10 μJ laser pulse energy. However, due to the defocusing effect of the plasma and the absorption of terahertz waves, as the laser intensity reaches a specific value, the intensity of THz radiation saturates [38]. In 2018, Thiele et al. demonstrated that the terahertz emission spectrum could be broadened due to plasmonic resonance controlled by the polarization of the elliptically shaped driving laser pulse [39].

2.2. Terahertz Amplifier

Currently, there are three types of THz amplifiers, including solid-state terahertz amplifiers (such as InP and GaN field-effect transistors) [40], waveguide-based traveling-wave terahertz amplifiers (TWAs) [41], and terahertz amplifiers based on photonics (such as laser-induced microplasma). Solid-state terahertz amplifiers have the disadvantage that the energy efficiency decreases with the increase in the operating frequency of the amplifier. Compared to the solid-state terahertz amplifiers, the microplasma can achieve higher-power amplification and higher operating frequency at higher efficiency.

Laser-induced plasma is used as an amplifier for terahertz wave propagation. In 2007, Dai et al. reported an amplification effect of THz wave in gases excited by femtosecond laser pulses caused by the four-wave-mixing parametric processes, as shown in Figure 5a [42]. In their experiment, a laser beam with a wavelength of 800 nm and its second harmonic is used to generate a nitrogen plasma. A seed THz wave is sent into the plasma with a length of 5 mm. When the total excitation intensity is 8×10^{14} W/cm^2, the amplification factor is 65%, as shown in Figure 5b.

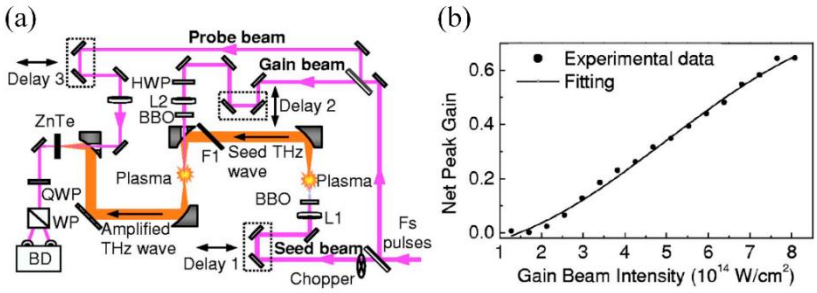

Figure 5. (**a**) Schematic diagram of laser-induced plasma amplification and detection of terahertz waves; (**b**) relationship curve between peak amplification factor and light excitation intensity [42].

In addition to the four-wave-mixing parametric processes, the effect of the negative absolute conductivity of plasma contributes to the amplification of the THz radiation in the plasma channel. Bogatskaya et al. analyzed and simulated the electron energy distribution function in the nitrogen, xenon, and argon plasma created by a femtosecond laser energy pulse. It is found that the plasma has to be highly nonequilibrium for THz amplification. Numerical results demonstrated that the amplification of the seed THz wave in the nonequilibrium Xe plasma channel up to several orders of magnitude is possible. The Xe plasma at atmospheric pressure is created by an intense femtosecond KrF laser pulse. The electron density of the Xe plasma is in the range of 10^{13}–10^{15} cm^{-3} [43–45].

Interestingly, Massood et al. demonstrated for the first time that the microplasma in the capillary could amplify the THz wave inside a meandering waveguide, which is helpful in terahertz traveling-wave amplifiers. A curved TE01 waveguide is coupled to the microplasma. The microplasma is confined within a silicon capillary with a thin dielectric coating on the inner surface wall. The usual size of the microplasma is in the range of 100–200 μm. The typical plasma density is 10^{10}–10^{14} cm^{-3}. The interaction between the plasma and the terahertz signal is coupled through electric dipoles. When the microplasma

phase and group velocities match that of the guided terahertz wave, the wave gains energy from the microplasma, and the terahertz signal gets amplified. Terahertz amplifiers based on microplasma instead of electron beam TWA have the following advantages: (1) thermionic emission required in e-beam generation can be replaced with gas ionization; (2) electrostatic lenses and magnetic focusing structures can be eliminated or reduced in complexity since plasmas can be self-focusing; (3) larger acceleration fields can be used by taking advantage of plasmas' space-charge electric fields of ~10^4–10^6 V/cm; (4) higher-power amplification at higher efficiency can be achieved. Their experimental results prove that the maximum amplification of the meandering waveguide with microplasma is about 12 dB at a frequency of 0.9 THz [46].

2.3. Terahertz Filter

The terahertz filter is one of the essential components in THz spectroscopy, imaging, and technology. It is used to selectively filter or efficiently extract terahertz signals for the improvement of the signal-to-noise ratio. Photonic crystals have photonic bandgaps, within which the propagation of THz waves is not permitted. It is usually used to confine and guide the THz wave propagation. To enhance the tunability of photonic bandgaps for THz wave modulation, plasma is introduced into the photonic crystals, forming an artificial periodic structured composition of plasma and dielectrics, known as a plasma photonic crystal (PPC). Compared to other methods based on the variety of external electric field, temperature, and pressure, the advantages of PPCs are wide tunability of the relative permittivity from negative to positive and rapid reconfiguration ability [12,18,47–50]. The PPCs used to modulate the THz wave propagation have been investigated recently.

In terms of THz PPC simulation, Elsami et al. investigated the characteristics of a microplasma photonic crystal for THz modulation [51]. Numerical results show that the characteristics of the PPC bandgaps depend on the incident angle of the terahertz wave, the electron density, and the thickness of the plasma layer. As the thickness of the plasma layer or plasma density increases, both the center frequency of the bandgap and the forbidden bandwidth decrease. Although these results show the possibility of microplasma photonic crystals for active terahertz filtering, the effects of collision frequency, discharge transient process, and the interaction between adjacent microplasma cells are ignored. In 2017, Kushner et al. considered the interaction between microplasma cells and simulated an open low-pressure surface microplasma array to modulate subterahertz wave propagation. It reveals that the diffusion of metastable atoms or ions between microplasma cells significantly impacts the subterahertz wave transmittance and the discharge characteristics of the microplasma [52]. In 2020, with the transfer matrix method, Wu et al. studied the effects of the collision frequency on the terahertz bandgap structure and transmission characteristics of a microplasma photonic crystal, as shown in Figure 6a. The increase in gas pressure leads to a decrease in the center frequency of the THz bandgap and the intensity of THz radiation. In Figure 6b, it is interesting to find that if the electron density is less than 10^{15} cm^{-3}, the center frequency and bandwidth of the first THz bandgap are almost unchanged. As the electron density further increases up to 10^{16} cm^{-3}, both the center frequency and bandwidth increase significantly [53]. What is more, Matthew et al. investigated the effects of plasma frequency, collision frequency, plasma column radius, lattice constant, and background dielectric permittivity on the subterahertz wave propagation with the plane wave expansion method. It is found that the radius of the microplasma cylinder and the background dielectric are the most effective control variables for the THz bandgap and its center frequency, respectively [54].

Previous works focused on the THz bandstop PPCs. If a defect layer is appropriately applied to the bandstop PPC, a THz passband PPC will occur. Wang et al. proposed a one-dimensional magnetized microplasma photonic crystal with a (AC)N(CBC)M(AC)N structure. A is the plasma layer with a 0.1–0.2 mm diameter, B is the dielectric defect layer, and C is the ordinary dielectric layer. N and M are the periods of the plasma layer and the dielectric defect layer, respectively. It is found that the width of each layer of A, B, and

C will affect the center frequency and transmission coefficient of the passband, but the width of the C layer has little effect on the transmission coefficient [55]. A flat passband is beneficial to the amplitude-frequency characteristic of the THz bandpass filter. It is interesting to observe that the number of photonic crystal cycles is beneficial to the flatness of the passband.

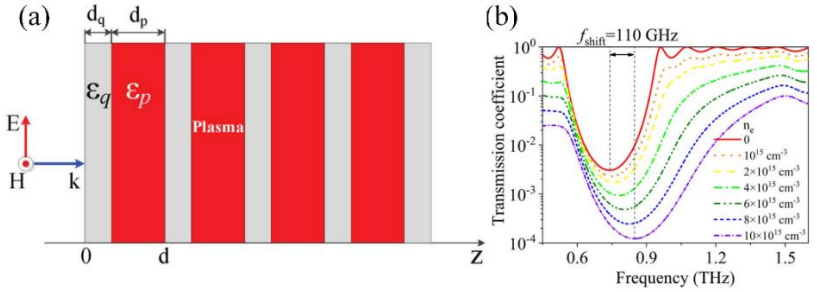

Figure 6. (**a**) Schematic diagram of one-dimensional collision microplasma photonic crystal; (**b**) relationship between the transmission coefficient of the first terahertz band gap and the frequency of the incident wave under different electron densities [53].

In terms of THz PPCs experiments, Sakai et al. reported a two-dimensional plasma photonic crystal based on hollow cathode discharge, as shown in Figure 7a. The electron density of the plasma is about 1×10^{13} cm^{-3}, the diameter of the plasma is 0.6 mm, and the lattice constant is 1.5 mm. A subterahertz bandgap around 0.1 THz is observed. The center frequency of the THz bandgap can be tuned by changing the lattice constant [56]. In 2017, Eden et al. developed a 5×10 microplasma jet array. The periodically aligned plasma jet and the surrounding air are the two dielectric types that form the two-dimensional microplasma photonic crystal. Each plasma jet has a diameter of 0.4 mm. The electron density is 3×10^{13} cm^{-3}. A narrow stopband at the center frequency of 157 GHz with a bandwidth of 1 GHz is observed for the first time. The maximum attenuation of THz radiation is only 5%, which is significantly different from the simulation results. One of the possible reasons is that the mixing of air and helium gas leads to the spatial nonuniformity of the collision frequency and plasma frequency [57]. Zhou et al. stated that the nonuniformity of plasma has a more significant impact on the propagation of terahertz waves in atmospheric microplasma [58]. The low electron density may also be responsible for the weak attenuation of THz radiation at the PPC stopband. Recently, Eden et al. further developed a three-dimensional plasma/metal/dielectric photonic crystal bandstop filter, as shown in Figure 8a. Two subterahertz stopbands at the center frequencies of 131 GHz and 138 GHz are obtained. When the electron density increases, the center frequency of the stopband increases [59]. Therefore, the simulation and experimental results above demonstrated that the microplasma photonic crystals served as THz filters are well suited to control the THz wave propagation.

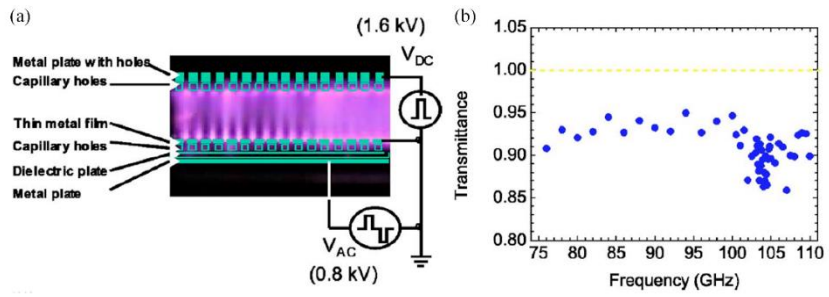

Figure 7. Microplasma column array and its filtering characteristic diagram. (**a**) Schematic diagram of the electrode structure with a lattice constant of 1.5 mm and the discharge diagram of the microplasma column array; (**b**) variation of millimeter-wave transmission coefficient with electromagnetic wave frequency in TE mode [56].

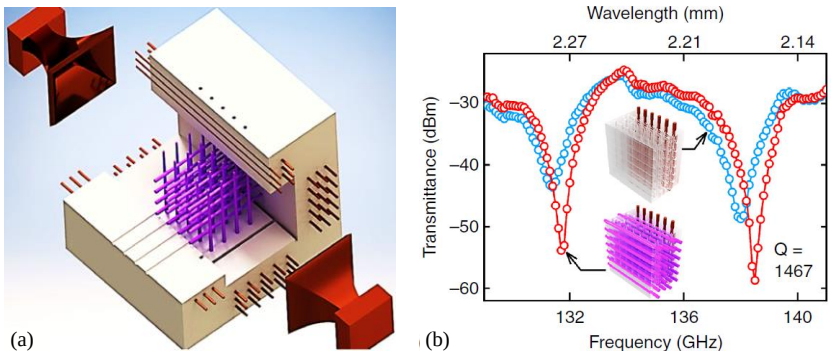

Figure 8. (**a**) Three-dimensional plasma/metal/dielectric photonic crystal band-stop filter; (**b**) The narrowing of the 138 GHz resonance line shape with the introduction of plasma to the crystal [59].

2.4. Terahertz Detector

The methods of terahertz wave detection are classified as incoherent detection and coherent detection. Incoherent detection is usually based on the thermal effect of detection materials on terahertz waves, which can be used to directly measure the intensity and average power of terahertz waves, such as bolometer, pyroelectric, and Golay cell [60]. These detectors can be applied to the power measurement of continuous terahertz wave and terahertz imaging. For the measurement of pulsed terahertz waves, the phase information of the pulse terahertz wave will be lost. On the other hand, coherent detection is usually applied to the measurement of pulsed terahertz waves, such as photoconductivity (PC) sampling and electro-optical sampling (FS-EOS) detectors [61]. The speed of PC sampling is limited by the resonant characteristic of the antenna structure. For FS-EOS detectors, the balance between the detection sensitivity and the frequency response is largely affected by the type and thickness of crystal materials. The thicker the electro-optic crystal is, the higher the detection sensitivity will be, but the detection bandwidth will be reduced. In addition to the above THz detectors, microplasma can also be applied to THz detection, which has an ultrawide detection bandwidth and high sensitivity compared to other types of THz detectors.

Laser-induced plasma in the air is an important approach to detect broadband THz waves. Dai et al. firstly demonstrated the coherent detection of broadband THz waves with ambient air. As shown in Figure 9, it is achieved by the E-field-induced second-harmonic generation from the third-order nonlinear optical process with femtosecond laser pulses, which can be applied to the temporal measurement of pulsed THz pulses. The coherent detection is limited to the cases in which the tunnel ionization process dominates in gases [62]. Liu et al. reported a detection method of THz pulses by the THz-enhanced emission of fluorescence from air plasma. The air plasma induced by a femtosecond laser has an electron density of 10^{14}–10^{15} cm^{-3}. The THz-enhanced fluorescence emission is caused by the electron heating and electron-impact excitation of air molecules or ions under the THz field [63]. Clough et al. observed a 10% acoustic enhancement from a laser-induced plasma under single-cycle THz radiation, providing a promising method for coherent THz wave remote detection. It is probably caused by the THz plasma heating through energy transfer from THz wave into translational motion of the gas molecules [64,65].

Due to the high complexity and high cost of the femtosecond laser-induced plasma system, a simple method of THz wave detection is required. Hou et al. firstly proposed a weakly ionized plasma detector for THz continuous wave. The dc neon plasma is generated in the electrode gap of 0.15 mm. As the discharge current increases, the responsivity of the THz detector increases firstly, reaches the peak of 194.4 V/W at 1.4 mA, and finally decreases [66]. Furthermore, a microplasma array is fabricated to detect the THz wave [67].

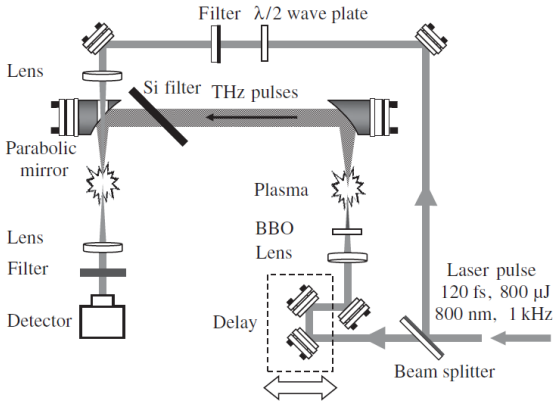

Figure 9. Schematic diagram of the coherent detection of broadband THz waves with ambient air [62].

3. Challenges

3.1. THz Radiation from Laser-Induced Microplasma

Regarding the mechanism of THz waves emitted from laser-induced microplasma, a photocurrent theory proposed by Kim's team is widely accepted [68]. They believed that the free electrons released by the ionization of gas molecules are driven by the asymmetric laser field, resulting in a fast transient current and emitting THz wave. On the other hand, Debayle et al. found that the THz radiation may originate from the plasma oscillation or photoionization, where the THz radiation intensity is dependent on the plasma skin depth and propagation length [69,70]. To understand the mechanism of the THz radiation from laser-induced microplasma, Kemp et al. and Sheng et al. made great efforts on the time-domain diagnostics and effective regulation of the terahertz radiation spectrum by the particle-in-cell (PIC) model [34,35,71–75]. Nevertheless, it is still unclear which mechanism of THz radiation is dominant in laser-induced microplasma. Moreover, the energy efficiency of the THz sources based on laser-induced microplasma is requires further improvement for THz applications in 6G communications and explosives detections.

3.2. The Amplification of THz Radiation by Microplasma

Regarding the amplification mechanism of THz radiation by microplasma, Dai et al. believed that four-wave-mixing parametric processes are the main reasons for amplification of THz radiation by laser-induced plasma. This is different from the explanation from Bogatskaya et al. that the negative absolute conductivity of laser-induced plasma should be responsible for the amplification. Moreover, Massood et al. proposed that the mechanism based on electric dipoles is attributed to amplifying THz wave inside a meandering waveguide by the microplasma in the capillary, where the microplasma is generated by electrical discharge instead of femtosecond laser energy pulses. Reference [44] reported that the relationship between the gain of terahertz wave amplification and the electron density is nonlinear. The amplification mechanism of THz radiation by microplasma is unclear yet, which will be solved in the near future.

3.3. Microplasma Photonic Crystals

Previous experimental works have demonstrated that some specially designed microplasma photonic crystals have THz stopbands at 0.1–0.2 THz, which could be used to control the THz wave propagation by changing plasma parameters. Simulation results have also predicted that THz radiation with frequency up to several THz can be tuned by microplasma photonic crystals as long as the plasma density increases to 10^{15} cm^{-3} or higher. Further experimental verification of this prediction is needed. In addition, the effects of the plasma uniformity, the transient discharge process, and the 3D complex structure on the THz bands of the microplasma photonic crystals are required to be investigated.

3.4. THz Detection by Microplasma

Previous works have demonstrated the detection methods of THz radiation from the aspects of second-harmonic generation, emission of fluorescence, and acoustic signals from laser-induced microplasma. The qualitative interpretations of the detection principles have been described. On the other hand, Hou et al. proposed a detection method of THz wave by microplasma or microplasma array, where the microplasma is achieved by glow discharge at low pressure. Although the effects of gas pressure, gas composition, and discharge current on the responsivity and stability of the THz detector have been studied, the measurement mechanism of this THz detector remains unclear yet.

4. Conclusions

The application of microplasma to THz functional devices from the aspects of terahertz sources, amplifiers, filters, and detectors is reviewed in this work. The conclusions are presented as follows.

(1) THz sources generated by the "one-color" and "two-color" methods are based on the laser-induced microplasma, where the microplasma has high electron density in the range of 10^{17} cm^{-3}–10^{19} cm^{-3}. The size of microplasma and the electron density greatly impact the optical-to-THz conversion efficiency. The THz sources have the advantages of a broad frequency spectrum and high power, which is very useful for identifying molecular crystals and biological macromolecules.

(2) In addition to the laser-induced microplasma, the microplasma in the capillary generated by gas discharge has proved helpful in amplifying the THz wave. It shows the possibility that the microplasma can be served as a THz amplifier, which has the advantages of high-power amplification at high efficiency. However, different amplification mechanisms based on four-wave-mixing parametric processes, the negative absolute conductivity of microplasma, and electric dipoles are proposed, which are needed to investigate in the future.

(3) Both experimental and simulation results demonstrated that microplasma photonic crystals have THz stopbands or passbands in the frequency range of 0.1–0.2 THz, which allows tuning the THz wave propagation by changing the plasma parameters. The THz filters based on the microplasma photonic crystals have advantages of fast response and reconfiguration ability. However, the control of THz wave propagation with frequency up to 1 THz or higher by microplasma photonic crystals needs further exploration.

(4) The detection methods of THz radiation, based on the second-harmonic generation, emission of fluorescence, and acoustic signals from laser-induced microplasma, have been developed and well studied. In addition, a simple detection method of THz radiation, based on the interaction between THz wave and the microplasma produced by glow discharge, is introduced. However, the detection mechanism of this method remains unknown at present.

In general, the microplasma technology successfully applied to the THz field, such as THz sources, amplifiers, filters, and detectors, opens a new area of exploration for both THz technology and plasma. It is beneficial to promote interdisciplinary research between them.

Author Contributions: Conceptualization, S.W. and L.Y.; writing—original draft preparation, Y.G. and X.L.; writing—review and editing, Y.G., S.W. and X.L.; visualization, Y.G.; supervision, S.W.; project administration, C.Z. and S.W.; funding acquisition, C.Z. and S.W. All authors have read and agreed to the published version of the manuscript.

Funding: This research was funded by the National Key Research and Development Program of China, Grant Number 2021YFF0603100, the National Natural Science Foundation of China, Grant Number 51977110, and Research on Evaluation Method of Overall Function and Effectiveness of Cable Fire Protection Products of Jiangsu Electric Power Research Institute of State Grid of China, Grant Number J2021137.

Institutional Review Board Statement: Not applicable.

Informed Consent Statement: Not applicable.

Data Availability Statement: Not applicable.

Conflicts of Interest: The authors declare no conflict of interest.

References

1. Liang, W.; Chao, T.; Zhu, S. Terahertz Time Domain Spectroscopy of Transformer Insulation Paper after Thermal Aging Intervals. *Materials* **2018**, *11*, 2124.
2. Dhillon, S.S.; Vitiello, M.S.; Linfield, E.H.; Davies, A.G.; Hoffmann, M.C.; Booske, J.; Paoloni, C.; Gensch, M.; Weightman, P.; Williams, G.P.; et al. The 2017 terahertz science and technology roadmap. *J. Phys. D Appl. Phys.* **2017**, *50*, 043001. [CrossRef]
3. Siegel, P.H. Terahertz technology in biology and medicine. *IEEE Trans. Microw. Theory Tech.* **2004**, *52*, 2438–2447. [CrossRef]
4. Siegel, P.H. THz technology. *IEEE Trans. Microw. Theory Tech.* **2002**, *50*, 910–928. [CrossRef]
5. Shi, S.C.; Paine, S.; Yao, Q.J.; Lin, Z.H.; Li, X.X.; Duan, W.Y.; Matsuo, H.; Zhang, Q.; Yang, J.; Ashley, M.C.B.; et al. Terahertz and far-infrared windows opened at Dome A in Antarctica. *Nat. Astron.* **2016**, *1*, 1. [CrossRef]
6. Hangyo, M. Development and future prospects of terahertz technology. *Jpn. J. Appl. Phys.* **2015**, *54*, 1–16. [CrossRef]
7. Jepsen, P.U.; Cooke, D.G.; Koch, M. Terahertz spectroscopy and imaging—Modern techniques and applications. *Laser Photonics Rev.* **2011**, *5*, 1–43. [CrossRef]
8. Son, J.H.; Oh, S.J.; Cheon, H. Potential clinical applications of terahertz radiation. *J. Appl. Phys.* **2019**, *125*, 190901. [CrossRef]
9. Shen, Y.C.; Lo, T.; Taday, P.F. Detection and identification of explosives using terahertz pulsed spectroscopic imaging. *Appl. Phys. Lett.* **2005**, *86*, 377. [CrossRef]
10. Akyildiz, I.F.; Jornet, J.M.; Chong, H. Terahertz band: Next frontier for wireless communications. *Phys. Commun.* **2014**, *12*, 16–32. [CrossRef]
11. Mittleman, D.M. Twenty years of terahertz imaging. *Opt. Express* **2018**, *26*, 9417. [CrossRef] [PubMed]
12. Wang, B.; Cappelli, M.A. A tunable microwave plasma photonic crystal filter. *Appl. Phys. Lett.* **2015**, *107*, 199902. [CrossRef]
13. Ginzburg, V.L. *The Propagation of Electromagnetic Waves in Plasma*; Science Press: Beijing, China, 1978.
14. Waldman, M.; Gordon, R.G. Generalized electron gas–Drude model theory of intermolecular forces. *J. Chem. Phys.* **1979**, *71*, 1340–1352. [CrossRef]
15. Sakai, O.; Tachibana, K. Plasmas as metamaterials: A review. *Plasma Sources Sci. Technol.* **2012**, *21*, 013001. [CrossRef]
16. Xu, L.L.; Tao, Z.Y.; Sang, T.Q. Thermally Tunable Narrow Band Filter Achieved by Connecting Two Opaque Terahertz Waveguides. *IEEE Photonics Technol. Lett.* **2017**, *29*, 869–872. [CrossRef]
17. Li, S.; Liu, H.; Sun, Q.; Huang, N.A. Tunable Terahertz Photonic Crystal Narrow-Band Filter. *IEEE Photonics Technol. Lett.* **2015**, *27*, 752–754. [CrossRef]
18. Xue, Q.W.; Wang, X.H.; Liu, C.L.; Liu, Y.W. Pressure-controlled terahertz filter based on 1D photonic crystal with a defective semi-conductor. *Plasma Sci. Technol.* **2018**, *20*, 035504. [CrossRef]
19. Federici, J.; Moeller, L. Review of terahertz and subterahertz wireless communications. *J. Appl. Phys.* **2010**, *107*, 6–323. [CrossRef]
20. Zhang, X.C.; Shkurinov, A.; Zhang, Y. Extreme terahertz science. *Nat. Photonics* **2017**, *11*, 16–18. [CrossRef]
21. Yu, J. Generation and Detection of Terahertz Signal. In *Broadband Terahertz Communication Technologies*; Springer: Singapore, 2021.
22. Shur, M. Terahertz technology: Devices and applications. In Proceedings of the 35th European Solid-State Device Research Conference, Grenoble, France, 16 September 2005.
23. Karpowicz, N.; Dai, J.; Lu, X.; Chen, Y.; Yamaguchi, M.; Zhao, H.; Zhang, X.-C. Coherent heterodyne time-domain spectrometry covering the entire "terahertz gap". *Appl. Phys. Lett.* **2008**, *92*, 011131. [CrossRef]
24. Liao, G.; Li, Y.; Zhang, Y. Demonstration of Coherent Terahertz Transition Radiation from Relativistic Laser-Solid Interactions. *Phys. Rev. Lett.* **2016**, *116*, 205003. [CrossRef] [PubMed]
25. Vvedenskii, N.V.; Korytin, A.I.; Kostin, V.A. Two-Color Laser-Plasma Generation of Terahertz Radiation Using a Frequency-Tunable Half Harmonic of a Femtosecond Pulse. *Phys. Rev. Lett.* **2014**, *112*, 055004. [CrossRef] [PubMed]
26. Lu, X.; Zhang, X.C. Generation of Elliptically Polarized Terahertz Waves from Laser-Induced Plasma with Double Helix Electrodes. *Phys. Rev. Lett.* **2012**, *108*, 123903. [CrossRef] [PubMed]
27. de Alaiza Martínez, P.G.; Babushkin, I.; Bergé, L.; Skupin, S.; Cabrera-Granado, E.; Köhler, C.; Morgner, U.; Husakou, A.; Herrmann, J. Boosting Terahertz Generation in Laser-Field Ionized Gases Using a Sawtooth Wave Shape. *Phys. Rev. Lett.* **2015**, *114*, 183901. [CrossRef] [PubMed]
28. Matsubara, E.; Nagai, M.; Ashida, M. Ultrabroadband coherent electric field from far infrared to 200 THz using air plasma induced by 10 fs pulses. *Appl. Phys. Lett.* **2012**, *101*, 021105. [CrossRef]
29. Hamster, H.; Sullivan, A.; Gordon, S. Subpicosecond, electromagnetic pulses from intense laser-plasma interaction. *Phys. Rev. Lett.* **1993**, *71*, 2725. [CrossRef] [PubMed]
30. Cook, D.J.; Hochstrasser, R.M. Intense terahertz pulses by four-wave rectification in air. *Opt. Lett.* **2000**, *25*, 1210–1212. [CrossRef] [PubMed]
31. Buccheri, F.; Zhang, X.C. Terahertz emission from laser-induced microplasma in ambient air. *Optica* **2015**, *2*, 366–369. [CrossRef]
32. Liu, K.; Buccheri, F.; Zhang, X.C. Terahertz science and technology of micro-plasma. *Physics* **2015**, *44*, 6.

33. Zhang, X.C.; Buccheri, F. Terahertz photonics of microplasma and beyond. *Lith. J. Phys.* **2018**, *58*, 248–256. [CrossRef]
34. Chen, M.; Yuan, X.; Sheng, Z. Scalable control of terahertz radiation from ultrashort laser-gas interaction. *Appl. Phys. Lett.* **2012**, *101*, 161908. [CrossRef]
35. Ding, W.J.; Sheng, Z.M. Sub GV/cm terahertz radiation from relativistic laser-solid interactions via coherent transition radiation. *Phys. Rev. E* **2016**, *93*, 063204. [CrossRef] [PubMed]
36. Wu, H.C.; Sheng, Z.M.; Dong, Q.L. Powerful terahertz emission from laser wakefields in inhomogeneous magnetized plasmas. *Phys. Rev. E* **2007**, *75*, 016407. [CrossRef]
37. Thiele, I.; Martinez, P.G.D.A.; Nuter, R. Broadband terahertz emission from two-color femtosecond-laser-induced microplasmas. *Phys. Rev. A* **2017**, *96*, 053814. [CrossRef]
38. Liu, K.; Koulouklidis, A.D.; Papazoglou, D.G. Enhanced terahertz wave emission from air-plasma tailored by abruptly autofocusing laser beams. *Optica* **2016**, *3*, 605–608. [CrossRef]
39. Thiele, I.; Zhou, B.; Nguyen, A. Terahertz emission from laser-driven gas plasmas: A plasmonic point of view. *Optica* **2018**, *5*, 1617–1622. [CrossRef]
40. Deal, W.R. Solid-state amplifiers for terahertz electronics. In Proceedings of the 2010 IEEE MTT-S International Microwave Symposium, Anaheim, CA, USA, 23–28 May 2010; pp. 1122–1125.
41. Tucek, J.C.; Basten, M.A.; Gallagher, D.A.; Kreischer, K.E. Testing of a 0.850THz vacuum electronic power amplifier. In Proceedings of the 2013 IEEE 14th International Vacuum Electronics Conference (IVEC), Paris, France, 21–23 May 2013; pp. 1–2.
42. Dai, J.; Xie, X.; Zhang, X.C. Terahertz wave amplification in gases with the excitation of femtosecond laser pulses. *Appl. Phys. Lett.* **2007**, *91*, 211102. [CrossRef]
43. Bogatskaya, A.V.; Volkova, E.A.; Popov, A.M. Plasma channel produced by femtosecond laser pulses as a medium for amplifying electromagnetic radiation of the subterahertz frequency range. *Quantum Electron.* **2013**, *43*, 1110. [CrossRef]
44. Bogatskaya, A.V.; Volkova, E.A.; Popov, A.M. On the possibility of a short subterahertz pulse amplification in a plasma channel created in air by intense laser radiation. *J. Phys. D Appl. Phys.* **2014**, *47*, 185202. [CrossRef]
45. Bogatskaya, A.V.; Gnezdovskaia, N.E.; Volkova, E.A. The role of plasma kinetics in the process of THz pulses generation and amplification. *Plasma Sources Sci. Technol.* **2020**, *29*, 105016. [CrossRef]
46. Tabib-Azar, M.; Fawole, O.C.; Pandey, S.S. Microplasma traveling wave terahertz amplifier. *IEEE Trans. Electron. Devices* **2017**, *64*, 3877–3884. [CrossRef]
47. Zhang, H.F.; Liu, S.B.; Kong, X.K. The properties of photonic band gaps for three-dimensional plasma photonic crystals in a di-amond structure. *Phys. Plasmas* **2013**, *20*, 042110. [CrossRef]
48. Guo, B.; Xie, M.Q.; Peng, L. Photonic band structures of one-dimensional photonic crystals doped with plasma. *Phys. Plasmas* **2012**, *19*, 072111. [CrossRef]
49. Zhang, L.; Ouyang, J.T. Experiment and simulation on one-dimensional plasma photonic crystals. *Phys. Plasmas* **2014**, *21*, 103514. [CrossRef]
50. Fan, W.; Zhang, X.; Dong, L. Two-dimensional plasma photonic crystals in dielectric barrier discharge. *Phys. Plasmas* **2010**, *17*, 113501. [CrossRef]
51. Askari, N.; Mirzaie, R.; Eslami, E. Analysis of band structure, transmission properties, and dispersion behavior of THz wave in one-dimensional parabolic plasma photonic crystal. *Phys. Plasmas* **2015**, *22*, 112117. [CrossRef]
52. Qu, C.; Tian, P.; Semnani, A. Properties of arrays of microplasmas: Application to control of electromagnetic waves. *Plasma Sources Sci. Technol.* **2017**, *26*, 105006. [CrossRef]
53. Shuqun, W.; Yuxiu, C.; Minge, L. Numerical study on the modulation of THz wave propagation by collisional microplasma photonic crystal. *Plasma Sci. Technol.* **2020**, *22*, 115402.
54. Paliwoda, M.C.; Rovey, J.L. Multiple parameter space bandgap control of reconfigurable atmospheric plasma photonic crystal. *Phys. Plasmas* **2020**, *27*, 023516. [CrossRef]
55. Wang, Y.; Liu, S.; Zhong, S. Tunable multichannel terahertz filtering properties of dielectric defect layer in one-dimensional magnetized plasma photonic crystal. *Opt. Commun.* **2020**, *473*, 125985. [CrossRef]
56. Sakaguchi, T.; Sakai, O.; Tachibana, K. Photonic bands in two-dimensional microplasma arrays. II. Band gaps observed in millimeter and subterahertz ranges. *J. Appl. Phys.* **2007**, *101*, 073305. [CrossRef]
57. Yang, H.J.; Park, S.J.; Eden, J.G. Narrowband attenuation at 157 GHz by a plasma photonic crystal. *J. Phys. D Appl. Phys.* **2017**, *50*, 43–50. [CrossRef]
58. Yao, J.; Yuan, C.; Li, H. 1D photonic crystal filled with low-temperature plasma for controlling broadband microwave transmission. *AIP Adv.* **2019**, *9*, 065302. [CrossRef]
59. Sun, P.P.; Zhang, R.; Chen, W. Dynamic plasma/metal/dielectric photonic crystals in the mm-wave region: Electromagnetically-active artificial material for wireless communications and sensors. *Appl. Phys. Rev.* **2019**, *6*, 041406. [CrossRef]
60. Rogalski, A. History of infrared detectors. *Opto-Electron. Rev.* **2012**, *20*, 279–308. [CrossRef]
61. Park, S.G.; Melloch, M.R.; Weiner, A.M. Comparison of terahertz waveforms measured by electro-optic and photoconductive sampling. *Appl. Phys. Lett.* **1998**, *73*, 3184–3186. [CrossRef]
62. Dai, J.; Xie, X.; Zhang, X.C. Detection of broadband terahertz waves with a laser-induced plasma in gases. *Phys. Rev. Lett.* **2006**, *97*, 103903. [CrossRef] [PubMed]

63. Liu, J.; Zhang, X.C. Terahertz-radiation-enhanced emission of fluorescence from gas plasma. *Phys. Rev. Lett.* **2009**, *103*, 235002. [CrossRef]
64. Clough, B.; Liu, J.; Zhang, X.C. Laser-induced photoacoustics influenced by single-cycle terahertz radiation. *Opt. Lett.* **2010**, *35*, 3544–3546. [CrossRef]
65. Clough, B.; Liu, J.; Zhang, X.C. "All air–plasma" terahertz spectroscopy. *Opt. Lett.* **2011**, *36*, 2399–2401. [CrossRef] [PubMed]
66. Hou, L.; Shi, W.; Chen, S. Terahertz continuous wave detection using weakly ionized plasma in inert gases. *IEEE Electron. Device Lett.* **2013**, *34*, 689–691. [CrossRef]
67. Hou, L.; Han, X.; Shi, W. Detecting terahertz waves using microplasma array. In Proceedings of the 2016 IEEE International Conference on Plasma Science (ICOPS), Banff, AB, Canada, 19–23 June 2016.
68. Kim, K.Y.; Glownia, J.H.; Taylor, A.J. Terahertz emission from ultrafast ionizing air in symmetry-broken laser fields. *Opt. Express* **2007**, *15*, 4577–4584. [CrossRef] [PubMed]
69. Li, N.; Bai, Y.; Miao, T. Revealing plasma oscillation in THz spectrum from laser plasma of molecular jet. *Opt. Express* **2016**, *24*, 23009–23017. [CrossRef] [PubMed]
70. Debayle, A.; Gremillet, L.; Berge, L. Analytical model for THz emissions induced by laser-gas interaction. *Opt. Express* **2014**, *22*, 13691–13709. [CrossRef]
71. Du, H.; Chen, M.; Sheng, Z. THz emission control by tuning density profiles of neutral gas targets during intense laser-gas interaction. *Appl. Phys. Lett.* **2012**, *101*, 18111318. [CrossRef]
72. Sheng, Z.M.; Mima, K.; Zhang, J. Emission of electromagnetic pulses from laser wakefields through linear mode conversion. *Phys. Rev. Lett.* **2005**, *94*, 0950039. [CrossRef] [PubMed]
73. Liao, G.Q.; Li, Y.T.; Li, C. Bursts of Terahertz Radiation from Large-Scale Plasmas Irradiated by Relativistic Picosecond Laser Pulses. *Phys. Rev. Lett.* **2015**, *114*, 25500125. [CrossRef] [PubMed]
74. Kemp, A.J.; Pfund, R.; Meyer-Ter-Vehn, J. Modeling ultrafast laser-driven ionization dynamics with Monte Carlo collisional particle-in-cell simulations. *Phys. Plasmas* **2004**, *11*, 5648–5657. [CrossRef]
75. Babushkin, I.; Kuehn, W.; Khler, C. Ultrafast Spatiotemporal Dynamics of Terahertz Generation by Ionizing Two-Color Femtosecond Pulses in Gases. *Phys. Rev. Lett.* **2010**, *105*, 053903. [CrossRef]